



# Mono- and Dinuclear 1-(2-Pyridyl)-4-phenyl-1,2,3-triazole-Based Ir(III) and Rh(III) Complexes

María Moreno-Latorre, María C de la Torre, Heinz Gornitzka, Catherine Hemmert, Miguel A Sierra

## ► To cite this version:

María Moreno-Latorre, María C de la Torre, Heinz Gornitzka, Catherine Hemmert, Miguel A Sierra. Mono- and Dinuclear 1-(2-Pyridyl)-4-phenyl-1,2,3-triazole-Based Ir(III) and Rh(III) Complexes. *Organometallics*, 2024, 43 (10), pp.1128 - 1136. 10.1021/acs.organomet.4c00079 . hal-04669053

**HAL Id: hal-04669053**

**<https://hal.science/hal-04669053v1>**

Submitted on 7 Aug 2024

**HAL** is a multi-disciplinary open access archive for the deposit and dissemination of scientific research documents, whether they are published or not. The documents may come from teaching and research institutions in France or abroad, or from public or private research centers.

L'archive ouverte pluridisciplinaire **HAL**, est destinée au dépôt et à la diffusion de documents scientifiques de niveau recherche, publiés ou non, émanant des établissements d'enseignement et de recherche français ou étrangers, des laboratoires publics ou privés.



Distributed under a Creative Commons Attribution 4.0 International License

# Mono- and Dinuclear 1-(2-Pyridyl)-4-phenyl-1,2,3-triazole-Based Ir(III) and Rh(III) Complexes

María Moreno-Latorre, María C. de la Torre,\* Heinz Gornitzka, Catherine Hemmert, and Miguel A. Sierra\*



Cite This: *Organometallics* 2024, 43, 1128–1136



Read Online

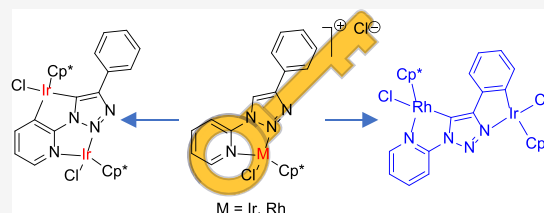
ACCESS |

Metrics & More

Article Recommendations

Supporting Information

**ABSTRACT:** The synthesis and characterization of a series of mono-, homo-, and heterobimetallic complexes involving iridium and rhodium centers have been achieved through the reaction of the proligand, 1-pyridyl-4-phenyl-1,2,3-triazole, and  $[M(Cp^*)Cl_2]_2$  ( $M = Ir, Rh$ ). The ligand undergoes coordination of the  $N,N$  fragment and subsequent  $N$ -directed C–H activation at the 1,2,3-triazole and phenyl or pyridyl moieties. Alternatively, direct  $N$ -directed C–H activation can be achieved. The structures of the prepared complexes were determined using spectroscopic techniques and confirmed by X-ray crystallography. The electrochemical properties of the complexes show a differentiate redox behavior between Ir–Ir centers and a clear influence of the second metal in heterobimetallic complexes. This flexible approach could have potential applications in catalysis and other areas of chemistry.



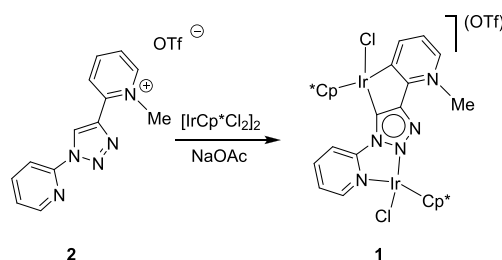
## INTRODUCTION

The selective functionalization of C–H bonds is a long-standing problem in chemistry. Methodologies based on transition metal complexes are still the most efficient and versatile of these transformations. The heteroatom directed C–H functionalization of aromatic rings is highly efficient in terms of selectivity.<sup>1</sup> Among the several systems used for this purpose, 1,2,3-triazole ligands having heterocycle chelating pendants<sup>2</sup> have been repeatedly studied. Thus, pyridine-1,2,3-triazole-based ligands are archetypical of these classes of compounds. The pyridine fragment may be located at carbon C4 or at nitrogen N1 of the 1,2,3-triazole ring, giving rise to the termed regular chelators (*reg*) **A** or inverse chelators (*inv*) **B**, respectively (Scheme 1). Regular chelators **A** coordinate through the more electron-rich nitrogen N3, while inverse chelators **B** coordinate through nitrogen N2.<sup>3</sup> Although both

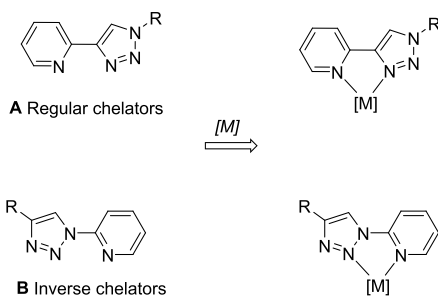
isomers (**A** and **B**) have been described, inverse chelators and their complexes are less common.<sup>4</sup>

The preparation of bimetallic complexes derived from a single 1,2,3-triazole ligand having two coordinating pendants has been scarcely studied. In fact, to the best of our knowledge, Albrecht reported the single example of a bimetallic complex of this type, namely, complex **1** derived from pyridinium salt **2**.<sup>5</sup> Complex **1** was prepared from  $[Ir(Cp^*)Cl_2]_2$  in the presence of NaOAc (Scheme 2).

## Scheme 2. Synthesis of a Bimetallic Complex **1** Having a 1,2,3-Triazole Ligand with Two Pendant Coordinating Moieties



## Scheme 1. Regular and Inverse Chelators Derived from 1,2,3-Triazoles



Received: February 27, 2024

Revised: April 9, 2024

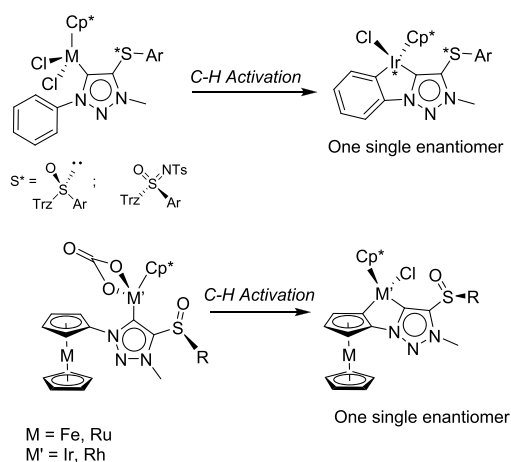
Accepted: April 26, 2024

Published: May 8, 2024



Our previous work in the chemistry of MIC-derived complexes<sup>6</sup> has led to the preparation of various enantiopure chiral at metal Ir(III) and Rh(III) complexes. This synthesis was achieved using enantiopure 1,2,3-triazolium salts derived from alkynylsulfoxides in the enantioselective-directed C–H metalation of an aromatic ring attached to the triazole CN1.<sup>7</sup> Subsequent work using these enantiopure 1,2,3-triazolium salts resulted in a sequence of chirality transfer from central (the sulfoxide) to metal (first C–H enantioselective functionalization forming a chiral at the metal half-sandwich moiety) to planar chirality (C–H activation of a ferrocene moiety) (Scheme 3).<sup>8</sup>

### Scheme 3. Synthesis of Homochiral Sulfoxide-Directed Enantiopure Complexes

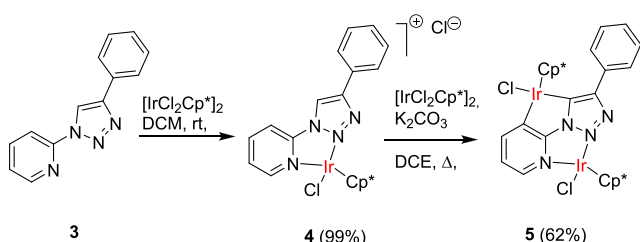


Based on these premises, we explored the use of easily available 1-pyridyl-4-phenyl-1,2,3-triazoles to prepare homo- and heteropolymetallic complexes. Reported here is the preparation of these novel new bimetallic complexes and their structural and electrochemical characterization. Zwitterionic bimetallic complex having two differently coordinated Ir centers will be described.

## RESULTS AND DISCUSSION

1-Pyridyl-4-phenyl-1,2,3-triazole **3** was obtained according to the literature procedure.<sup>9</sup> Treatment of **3** with 0.5 equiv of  $[\text{IrCp}^*\text{Cl}_2]_2$  in dichloromethane (DCM) at rt afforded after 18 h pure complex **4** in nearly quantitative yield (Scheme 4). The <sup>1</sup>H NMR of complex **4** showed signals for five H corresponding to the aromatic ring, four H assignable to the pyridyl moiety and one triazolyl hydrogen, in a pattern similar to the free ligand **3**, with the expected shifts due to the coordination of the Ir fragment. In addition, one signal singlet (15H) assignable to the pentamethylcyclopentyl ring ( $\text{Cp}^*$ )

### Scheme 4. Synthesis of Complexes **4** and **5**



confirms the incorporation of the  $[\text{IrClCp}^*]$  fragment to **3** (see Experimental Section). These data suggest that Ir coordinated both the triazole N2 and the pyridine nitrogen. In fact, the triazole proton shifts from 8.80 ppm in ligand **3** (measured in  $\text{DMSO}-d_6$ ) to 11.22 ppm (measured in  $\text{CDCl}_3$ ) in complex **4**. This strong downfield shift agreed with the proposed structure of complex **4**. The downfield shift of the CH in the 1,2,3-triazole ring is analogous to the one observed in the formation of 1,2,3-triazolium salts, which support the coordination of the 2-nitrogen of the 1,2,3-triazole moiety.

Next, complex **4** was reacted with 0.5 equiv of  $[\text{IrCl}_2\text{Cp}^*]_2$  in refluxing dichloroethane (DCE) in the presence of  $\text{K}_2\text{CO}_3$ . After 18 h of reaction, complex **5** was obtained in 62% yield (Scheme 4). The structure of complex **5** was determined by spectroscopic and spectrometric means. First, the appearance of two signal singlets in the <sup>1</sup>H NMR spectra attributable to two different  $[\text{Ir}(\text{Cp}^*)]$  units unequivocally confirms the presence of two nonequivalent  $[\text{IrClCp}^*]$  moieties ( $\delta\text{H}$  1.79 and 1.59 ppm, 15H each). Moreover, no signals for the triazole proton appeared, while three signals corresponding to 3H of the pyridine ring in ligand **3** were present, and the phenyl hydrogens remained unaltered. These data suggest the formation of a half-sandwich metallacycle by C–H activation between the C3 of the pyridine and the C5 of the 1,2,3-triazole rings. No metallacycles derived from the phenyl C–H ring activation were detected in this reaction. It is notable that although bimetallic complex **5** has two chiral Ir centers, only one diastereomeric racemate was obtained. A single crystal of complex **5** was obtained by crystallization from DCM/hexane. The structure of complex **5** was unambiguously established by an X-ray diffraction analysis (Figure 1). The two iridium atoms

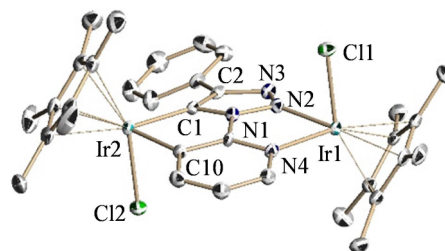


**Figure 1.** X-ray structure of complex **5** depicted as an ellipsoid plot at a 50% level. Selected bond lengths (Å) and angles [°]: Ir1–Cl1 2.406(2), Ir2–Cl2 2.408(2), Ir1–N2 2.100(6), Ir1–N4 2.137(7), Ir2–C1 2.049(7), Ir2–C10 2.073(7), N1–N2 1.335(8), N2–N3 1.316(9), N3–C2 1.374(9), C1–C2 1.417(10), C1–N1 1.340(9), N2–Ir1–N4 77.7(2), N2–Ir1–Cl1 87.7(2), N4–Ir1–Cl1 85.3(2), C1–Ir2–C10 80.4(3), C1–Ir2–Cl2 85.6(2), C10–Ir2–Cl2 88.2(2).

form a tetracyclic system with the deprotonated triazole and the deprotonated pyridine substituent. This tetracyclic system is nearly perfectly planar with a mean deviation of the best plane formed of only 0.082 Å. As depicted in Figure 1, the obtained diastereomer has the two  $\text{Cp}^*$  rings in relative *anticonfiguration* with respect to the plane defined by the bimetal-tetracyclic system. Therefore, the metalation reaction proceeds in a complete regio and diastereoselective manner.

Bimetallic iridium complex **5** deserves some additional comments. The complex is neutral, and the computed NBO charges of both centers were nearly identical (Figure 2).<sup>10</sup> Therefore, complex **5** may be described as a zwitterionic complex having a positive Ir-center (the one complexed by two strong  $\sigma$ -donor carbon ligands) and a negative Ir-center (the

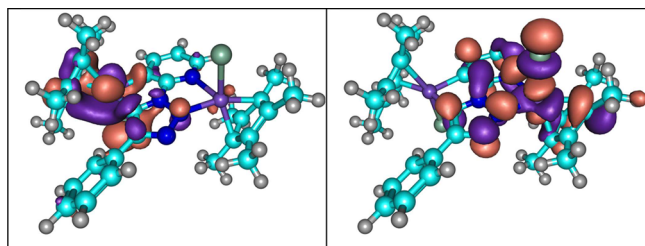


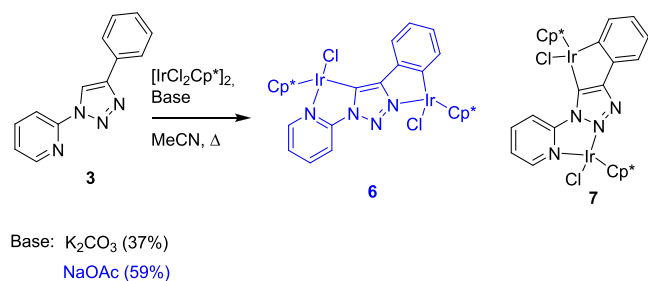
**Figure 2.** HOMO (left) and LUMO (right) of complex 5.

one coordinated to the less electron donor *N,N* ligand). The HOMO orbital is located in the C–Ir–C moiety, while the LUMO orbital is located in the N–Ir–N moiety. The initial coordination of the Ir to the *N,N* moiety of the 1-pyridyl-1,2,3-triazines moiety undoubtedly is responsible for the second coordination of the Ir to the C5 of the 1,2,3-triazine and the 3-CH of the phenyl group, probably by strongly increasing the acidity of the hydrogen at the C5 carbon of the 1,2,3-triazine ring.

The increased acidity of the hydrogen at the C5 carbon of the 1,2,3-triazine ring in complex 4 with respect to the proligand 3 is supported by the strong deshielding of this hydrogen. Thus, as indicated above, this hydrogen appears at 8.80 ppm in the  $^1\text{H}$  NMR spectra of proligand 3 and at 11.22 ppm in the  $^1\text{H}$  NMR spectra of complex 4. This  $\Delta\delta = 2.4$  ppm corresponds to a decrease of  $\approx 7.6$  units of  $\text{p}K_{\text{a}}$  upon Ir complexation.<sup>11</sup>

1,2,3-Triazole 3 was next treated with one equivalent of  $[\text{IrCp}^*\text{Cl}_2]_2$  in boiling acetonitrile and in the presence of  $\text{K}_2\text{CO}_3$  (Scheme 5). A new neutral bimetallic complex was

#### Scheme 5. Synthesis of Bimetallic Ir-Complex 6



obtained in a 37% yield. By switching the base to NaOAc, the yield of this product increased to 59%. Analogously to complex 3, the  $^1\text{H}$  NMR spectrum for the new compound showed two singlet signals attributable to two inequal  $\text{Cp}^*$  rings, as well as the disappearance of the triazole proton. In addition, signals corresponding to the four protons of the pyridine ring were clearly identified, but only four signals (two doublets and two triplets) attributable to the four hydrogens of the phenyl ring were observed. With these data, two possible structures 6 or its isomer 7 can be proposed for the new bimetallic complex (Scheme 5).

X-ray structural analysis unambiguously established structure 6 for the new bimetallic complex (Figure 3). Again, the metalation process was regio and diastereoselective. Now, one iridacycle formed involves the nitrogen of the pyridine and the C1 of the 1,2,3-triazole moiety, while the other one is formed from coordination of N3 of the 1,2,3-triazole and the *o*-carbon of the phenyl ring. The alternative structure of 7 has not been detected under any reaction conditions. Ir1 is only

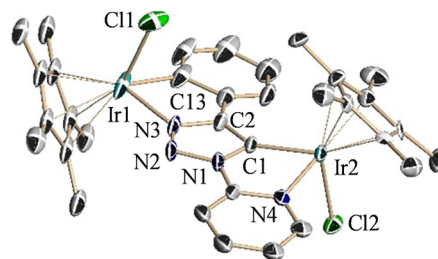


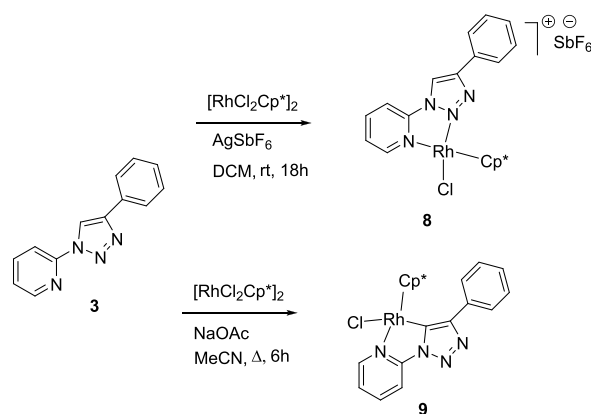
**Figure 3.** X-ray structure of Ir bimetallic complex 6 depicted as an ellipsoid plot at the 30% level. Noncoordinating  $\text{CHCl}_3$  molecules are omitted for clarity. Selected bond lengths [Å] and angles [°]: Ir1–Cl1 2.390(4), Ir2–Cl2 2.390(5), Ir1–N3 2.046(12), Ir1–C13 2.027(18), Ir2–C1 2.020(11), Ir2–N4 2.072(12), N1–N2 1.345(13), N2–N3 1.308(17), N3–C2 1.373(17), C1–C2 1.396(19), C1–N1 1.365(18), N3–Ir1–C13 78.2(6), N3–Ir1–Cl1 83.0(3), C13–Ir1–Cl1 87.9(4), C1–Ir2–N4 77.0(5), C1–Ir2–Cl2 93.5(4), N4–Ir2–Cl2 87.0(4).

0.18 Å out of the plane formed by N3–C2–C8 and C13, while Ir2 is clearly out of the plane formed by C1 N1 C3 and N4 with a distance of 0.39 Å in respect to this plane.

Both complexes 5 and 6 are bimetallic pentacyclic systems, but their origins are clearly different. Thus, while complex 5 is formed by the initial *N,N'*-coordination of Ir to 1,2,3-triazolepyridine system followed by double C–H activation of both the pyridine C3 and the H5 of the 1,2,3-triazole heterocycle, complex 6 derives from the nitrogen-directed (both pyridine and N3 of the 1,2,3-triazole ring) double CH activation of the aromatic and heteroaromatic rings. As indicated above, probably, the initial coordination of Ir to the *N,N* system of the pyridine and the 1,2,3-triazole ring determines the fate of the second Ir reaction by strongly increasing the acidity of the H5 of the 1,2,3-triazole ring, leading in these conditions to the observed complex 5. It is therefore foreseeable that complex 6 would be formed from complex 5 by initial decoordination of the Ir moiety followed by sequential N-directed C–H activation.

To further expand the scope of these metalation processes, ligand 3 was reacted with 0.5 equiv of  $[\text{RhCp}^*\text{Cl}_2]_2$  in DCM at rt in the presence of  $\text{AgSbF}_6$ .<sup>12</sup> Complex 8 was obtained in 92% yield in these conditions (Scheme 6).  $^1\text{H}$ - and  $^{13}\text{C}$ -NMR spectra showed a signal pattern almost identical to those of Ir-complex 4. In addition, HRMS analysis yielded a molecular

#### Scheme 6. Preparation of Mononuclear Rh-Complexes 8 and 9





peak accounting for the molecular formula  $C_{23}H_{25}ClN_4Rh$  corresponding to the monorhodium complex **8** (Scheme 6).

Subsequently, 1,2,3-triazole **3** was treated with 0.5 equiv of  $[RhCp^*Cl]_2$  in refluxing acetonitrile, in the presence of NaOAc to promote the C–H insertion. However, no reaction was observed after 18 h under these conditions. By increasing the amount of  $[RhCp^*Cl]_2$  to 1.0 equiv, mononuclear complex **9** was obtained in 70% yield, as evidenced by HRMS and  $^1H$  NMR data. Both the  $^1H$  NMR and HRMS confirmed the presence of only one  $Cp^*$  ring in the molecule ( $\delta H$  1.50 ppm, 15H;  $\delta C$  9.45 ppm,  $5CH_3$ ). In addition, the  $^1H$  NMR spectra of complex **9** lack the singlet signal characteristic of the triazole ring of the free ligand **3**. These data agree with structure **9** in which Rh has been inserted in the C5 C–H bond of the 1,2,3-triazole moiety. Finally, X-ray analysis confirmed unambiguously the structural hypothesis for complex **9** (Figure 4).

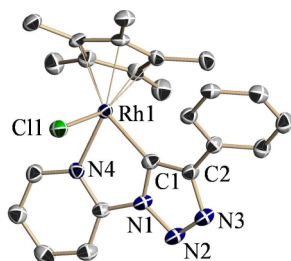
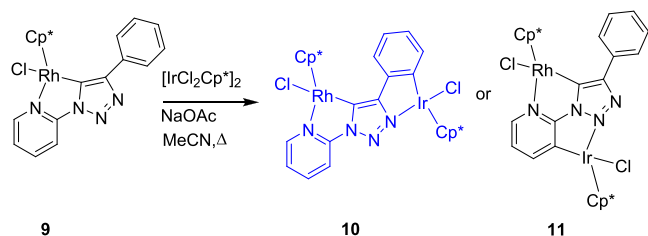


**Figure 4.** X-ray structure of mononuclear Rh-complex **9** depicted as an ellipsoid plot at a 50% level. Only one of two independent molecules in the asymmetric unit is shown. Selected bond lengths [Å] and angles [°]: Rh1–Cl1 2.391(1), Rh1–C1 2.025(4), Rh1–N4 2.100(3), N1–N2 1.370(5), N2–N3 1.299(5), N3–C2 1.387(5), C1–C2 1.389(5), C1–N1 1.363(5), C1–Rh1–N4 77.7(2), C1–Rh1–Cl1 90.1(2), N4–Rh1–Cl1 87.2(1).

Unfortunately, the synthesis of homobimetallic complexes analogous to complexes **5** and **6** was not possible, either using ligand **3** or complexes **8** and **9** as starting materials. The different reaction conditions tested, which include different solvents, stoichiometries, and reagents ratios, were unsuccessful, leading either to recovering unaltered materials or complex reaction mixtures.

The preparation of heterobimetallic Ir–Rh-complexes turned out to be challenging. Thus, Ir-complex **4** was reacted with  $[RhCp^*Cl_2]_2$  under different reaction conditions that favor C–H activation ( $K_2CO_3$ , boiling DCE, or NaOAc in refluxing MeCN). None of these conditions produced the desired bimetallic complexes. In contrast, treatment of Rh-complex **9** with  $[IrCp^*Cl_2]_2$  in the presence of NaOAc in boiling MeCN produced a new heterobimetallic complex **10** (Scheme 7) isolated as an orange solid in 43% yield. HRMS in the positive mode allows the identification of a molecular peak at 821.1447 uma, accounting for a molecular formula

#### Scheme 7. Synthesis of Heterobimetallic Complex **10**



$C_{33}H_{38}ClIrN_4Rh$ , that proves the presence of Rh and Ir in the complex. In fact, the  $^1H$  and  $^{13}C$  NMR spectra showed signals for two unequal  $Cp^*$  fragments. With these data structures, **10** and **11** (Scheme 7) are possible. The comparison of the  $^1H$  NMR spectrum of the new heterobimetallic complex with those of the bis-iridium complexes **5** and **6** makes evident that the pattern for the aromatic hydrogens of the new complex and compound **6** are similar (Figure 5). Thereof, we propose structure **10** for the Rh–Ir bimetallic complex.

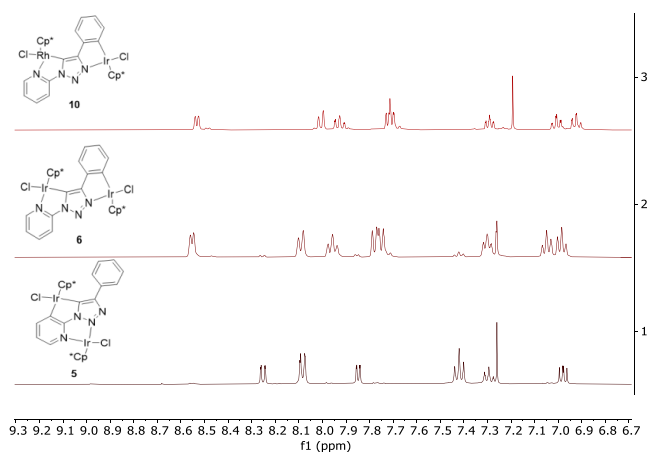


**Figure 5.** Comparative  $^1H$  NMR spectra of compounds **5**, **6**, and **10**.

**Electrochemistry.** The electrochemistry of complexes **4** and **8** was next studied. Ir-complex **4** and Rh-complex **8** show clear reduction waves at  $-1.21$  and  $-1.13$  V that are congruent to the two electron  $M(III)$  to  $M(I)$  reduction ( $M = Ir$  and  $Rh$ , respectively)<sup>13</sup> (Figure 6 and Table 1). Additionally, Ir(III)

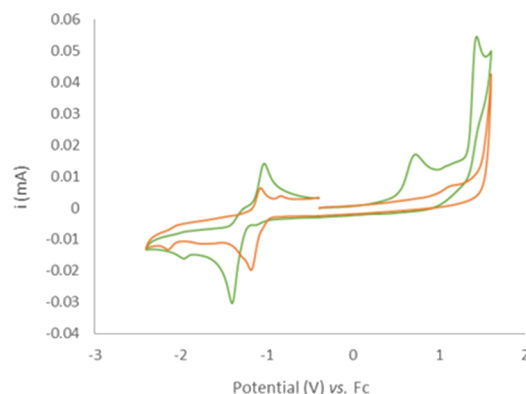


**Figure 6.** Cyclic voltammogram of complexes **4** and **8** in MeCN solution ( $10^{-3}$  M/ $[Bu_4N]PF_6$  0.1 M) at 0.1 V/s referred to  $Fc^+/Fc^0$ .

complex **4** shows an irreversible oxidation at 0.76 V wave attributable to the Ir(III) to Ir(IV) oxidation, while the additional wave observed for this complex should be a ligand oxidation event.<sup>14</sup>

The zwitterionic complex **5** exhibits three irreversible oxidation waves at 0.36, 0.89, and 1.13 V. According to the HOMO (Figure 2) of this complex, the first oxidation (with a strong cathodic shift compared to complex **4**) must correspond to the oxidation of Ir(III)/Ir(V) of the C,C-coordinated Ir-center. By analogy with complex **4**, the second oxidation wave should correspond to the oxidation of the N,N-coordinated-Ir-

Table 1. Electrochemical Data of Complexes 4–10

compound	$E^{ox}$	$E^{red}$	$E_{1/2}^{red}$
4	0.76	−1.01 <sup>a</sup>	−1.21
	1.46	−1.40 <sup>a</sup>	
5	0.36	−1.90	
	0.89		
	1.13		
6	0.41	−2.07	
	0.87		
	1.04		
8	1.17	−1.07 <sup>a</sup>	−1.13
		−1.18 <sup>a</sup>	
		−2.13	
9	0.97	−1.56 <sup>a</sup>	−1.65
	1.21	−1.73 <sup>a</sup>	
10	0.40	−1.65	
	0.96	−1.86	
	1.22		

<sup>a</sup>Quasireversible

center, while the third wave at 1.13 V should correspond to a ligand oxidation. Analogous to the oxidation process, the reduction wave is strongly shifted toward the cathode (−1.90 V), and according to the LUMO, it must correspond to the reduction of the N,N-coordinated Ir-center. The strong shifts observed in both oxidation and reduction events are justified by a considerable increase in the electronic density of the involved centers due to the zwitterionic nature of the system.

Complex **6** has a voltammogram similar to that of complex **5** (Figure 7). The analysis of the frontier orbitals (Figure 8) of

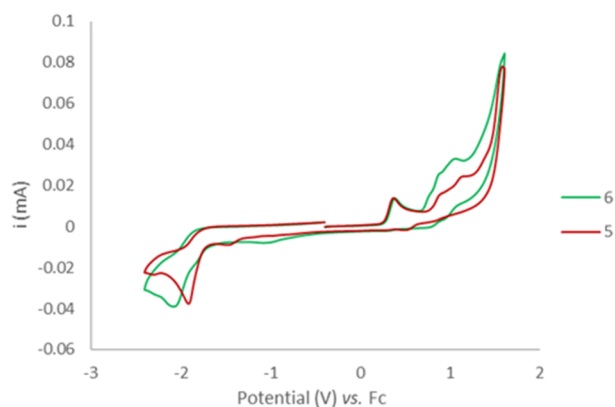


Figure 7. Cyclic voltammogram of complexes **5** and **6** in MeCN solution ( $10^{-3}$  M/[Bu<sub>4</sub>N]PF<sub>6</sub> 0.1 M) at 0.1 V/s referred to as Fc<sup>+</sup>/Fc<sup>0</sup>.

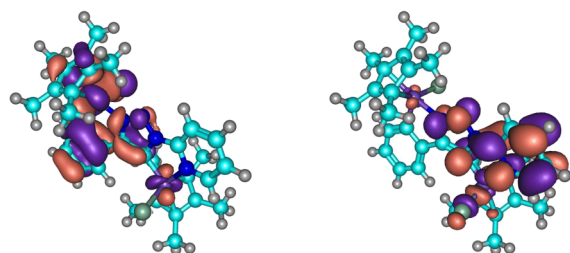


Figure 8. HOMO (left) and LUMO (right) from the homobimetallic complex **6**.

complex **6** explains this similar behavior with the Ir(III) C,N-bound to the triazole nitrogen and the phenyl ring oxidizing first and, again by analogy, the second and third oxidation waves corresponding to the additional Ir(III) atom and the ligand. The strong cathodic shift of the reduction (−2.07 V) indicates a strong increase in the electronic density of the metal atoms of the complex. This wave is shared between the Ir(III) bound to the MIC and the pyridine and 1,2,3-triazole ligands.

Finally, the heterobimetallic complex **10** exhibits electrochemical behavior similar to **6** in the oxidation section, with three oxidation waves (0.40, 0.96, and 1.22 V) due to the Ir fragment (Figure 9). Complex **10** shows two reduction waves.

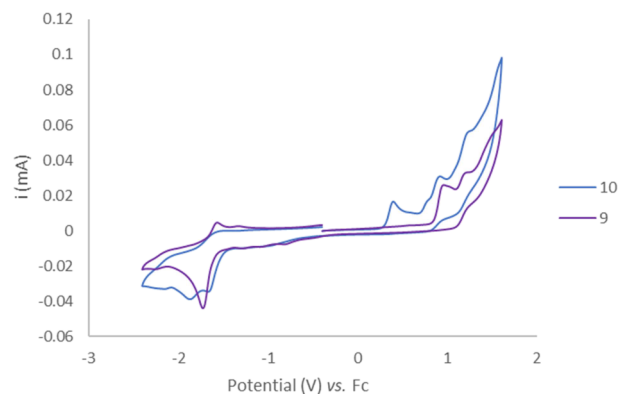


Figure 9. Cyclic voltammogram of complexes **9** and **10** in MeCN solution ( $10^{-3}$  M/[Bu<sub>4</sub>N]PF<sub>6</sub> 0.1 M) at 0.1 V/s referred to Fc<sup>+</sup>/Fc<sup>0</sup>.

The first reduction wave (−1.65 V) is attributable to the reduction of the Rh(III) center with ligand participation according to the LUMO of this complex represented in Figure 10 and the voltammogram of complex **10**. The second wave at

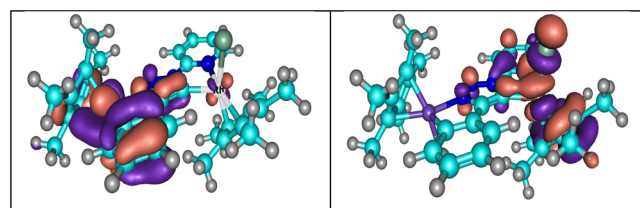


Figure 10. HOMO (left) and LUMO (right) from heterobimetallic complex **10**.

−1.86 V is strongly displaced toward the cathode with respect to the analogous wave of complexes **5** and **6** (see Table 1). This is due to the strong electron withdrawing exerted by the Rh(III) center.<sup>15</sup>

## CONCLUSIONS

The synthesis and characterization of several monometallic, homo- and heterobimetallic complexes of Ir and Rh from 1-(2-pyridyl)-1,2,3-triazoles have been accomplished. Several coordination modes with or without C–H activation have been obtained depending on the reaction conditions. The key for these processes is the formation of the cationic monometallic complexes of Ir(III), **4**, and Rh(III), **9**, in which the metal coordination occurs through the nitrogen of the pyridine and the N2 of the triazole ring. The generation of these complexes results in a deshielding of the signal

corresponding to the triazole proton by about 2 ppm, which derives from a strong increase in the acidity of the H5 of the 1,2,3-triazole ring. The reaction of the cationic monometallic complex **4** with  $[\text{IrCl}_2\text{Cp}^*]_2$  in DCE at reflux leads to a neutral bimetallic compound **5** where the 1,2,3-triazole coordinates with a  $\text{CpIrCl}$  unit as a bidentate  $N,N'$ -chelate and the other as a bidentate  $C,C'$ -ligand. Complex **5** can be described as having a zwitterionic structure in which one Ir nucleus would be positively charged, while the other Ir would be negatively charged.

When the reaction between proligand **3** and  $[\text{IrCl}_2\text{Cp}^*]_2$  was carried out in MeCN at reflux, bimetallic complex **6** was obtained. Complex **6** has one Ir coordinated between the nitrogen of the pyridine and the C5 of the 1,2,3-triazole and the second Ir complexes with the N3 of the triazole ring activating the CH of the phenyl ring. This double  $N$ -directed  $C-H$  activation is totally regio- and diastereoselective.

Interestingly, while the reaction of the 1,2,3-triazole **3** with  $[\text{RhCl}_2\text{Cp}]_2$  in the presence of  $\text{AgSbF}_6$  yielded the cationic Rh(III) complex **8**, the analogous reaction in the presence of a base ( $\text{NaOAc}$ ) yielded the complex **9** in which the Rh activated H5 of the 1,2,3-triazole moiety. Rh-bimetallic complexes analogous to Ir complexes **5** and **6** could not be obtained under the different conditions tested. Nevertheless, starting with complex **9**, the heterobimetallic complex **10** analogous to complex **6** was obtained in 43% yield.

The formation of the different products is directly related to the increase in the acidity of the hydrogen on C5 that causes the metal coordination to the  $N,N'$  fragment. This increase in acidity subsequently promotes the remaining CH activation reactions directed by the activation of the CH on C5 of the 1,2,3-triazole.

The electrochemistry of the prepared complexes demonstrates that the introduction of a second metal causes drastic changes in the position of the oxidation waves (a strong cathodic shift) as well as the reduction waves (an analogous shift) compared to complexes **4** and **8** in which the metal is coordinated to the nitrogens of the 1,2,3-triazole and the pyridine. This is consistent with the higher donating capacity of the NHC and  $C-M$  ( $M = \text{Ir}, \text{Rh}$ ) ligands in complexes **5**, **6**, and **10**. The analysis of the HOMO and LUMO of these complexes allows observing a similar behavior in the series of bimetallic complexes prepared, with the more easily oxidizable metal center being the one in which the MIC ligand does not participate. By contrast, the reduction occurred in the electron deficient moiety, the one attached to the MIC ligands.

Subsequent results on the use of these ligands in catalysis will be reported in due time.

## EXPERIMENTAL SECTION

**General Methods.** Unless noted otherwise, all manipulations were carried out under an argon atmosphere using standard Schlenk techniques. DMF, toluene,  $\text{CH}_2\text{Cl}_2$ , and  $\text{CH}_3\text{CN}$  were dried by passage through solvent purification columns containing activated alumina. Other solvents were HPLC grade and were used without purification. All reagents were obtained from commercial sources and used without additional purification unless noted otherwise. Flash column chromatography was performed using silica gel 60 (Merck,  $n^\circ$  1.09385, 230–400 mesh).  $^1\text{H}$  and  $^{13}\text{C}$  NMR spectra were recorded at 400 or 500 MHz ( $^1\text{H}$  NMR) and at 100 or 126 MHz ( $^{13}\text{C}$  NMR) using  $\text{CDCl}_3$  or acetonitrile- $d_3$  as solvents with the residual solvent signal as internal reference ( $\text{CHCl}_3$  7.26 and 77.2 ppm) (acetonitrile 1.94, 118.26, and 1.32 ppm). The following abbreviations are used to describe peak patterns when appropriate: s (singlet), d (doublet), t

(triplet), q (quadruplet), m (multiplet), and br (broad). The NMR peak assignments were based on the analysis of  $^1\text{H}$ – $^{13}\text{C}$ –HMBC and HSQC recorded spectra along with previously reported data for related compounds. High-resolution mass spectrometry (HRMS) by the ESI technique was performed with an Agilent 6500 accurate mass apparatus with a Q-TOF analyzer. IR spectra were recorded on a PerkinElmer 681 spectrophotometer. 2-Azidopyridine was prepared following the reported method.<sup>16</sup> The remaining starting materials were obtained from commercial sources and used without further purification.

**Computational Details.** All calculations were performed at the DFT level in vacuo using the B3LYP functional<sup>17</sup> as implemented in Gaussian16<sup>18</sup> supplemented with the Grimme's dispersion correction D3<sup>19</sup> and the def2-SVP basis set.<sup>20</sup>

**Preparation of Proligand 3.** Compound **3** was prepared following a modified literature procedure.<sup>21</sup> A mixture of 2-azidopyridine (300 mg, 2.5 mmol, 1 equiv), phenylacetylene (255 mg, 2.5 mmol, 1 equiv), and  $(\text{CuOTf})_2 \cdot \text{C}_6\text{H}_6$  (189 mg, 0.375 mmol, 0.15 equiv) in toluene (16 mL) was refluxed under argon until completion of the reaction (TLC analysis). The mixture was extracted with  $\text{CH}_2\text{Cl}_2$  three times. The organic layer was dried over  $\text{MgSO}_4$  and filtered. The solvent was removed under a vacuum. The crude product was purified by  $\text{SiO}_2$  column chromatography (hex:AcOEt, 1:1) to afford the pure triazole (**422** mg, 76%).  $^1\text{H}$  NMR (300 MHz,  $\text{CDCl}_3$ )  $\delta$  8.80 (s, 1H), 8.54–8.49 (m, 1H), 8.24 (d,  $J = 8.3$  Hz, 1H), 8.01–7.81 (m, 3H), 7.58–7.39 (m, 2H), 7.44–7.26 (m, 2H).

**Preparation of Ir-Complex 4.** To a solution of 60.0 mg (0.27 mmol, 1 equiv) of triazole **3** in  $\text{CH}_2\text{Cl}_2$  (5 mL) was added 107.6 mg (0.135 mmol, 0.5 equiv) of  $[\text{IrCl}_2\text{Cp}^*]_2$ . The reaction mixture was stirred under argon at room temperature for 18 h. The solvent was removed under vacuum, and the resulting residue was solved in the minimum amount of  $\text{CHCl}_3$  and precipitated with MeCN. The solvents were decanted, and the solid was washed with cold MeCN ( $\times 3$ ) and vacuum-dried to yield pure complex **4** as a yellow solid (165.8 mg, 99%).  $^1\text{H}$  NMR (400 MHz,  $\text{CDCl}_3$ )  $\delta$  11.22 (s, 1H), 9.53 (d,  $J = 8.0$  Hz, 1H), 8.66 (d,  $J = 4.9$  Hz, 1H), 8.35 (t,  $J = 7.5$  Hz, 1H), 8.11 (d,  $J = 7.4$  Hz, 2H), 7.67 (m, 1H), 7.45 (t,  $J = 7.3$  Hz, 2H), 7.39 (m, 1H), 1.77 (s, 15H).  $^{13}\text{C}$  NMR (101 MHz,  $\text{CDCl}_3$ )  $\delta$  151.6 (C), 149.9 (CH), 146.3 (C), 144.3 (CH), 129.9 (CH), 129.2 (2CH), 128.5 (C), 127.4 (CH), 126.6 (2CH), 124.7 (CH), 117.7 (CH), 90.2 (SC,  $\text{Cp}^*$ ), 9.1 (5 $\text{CH}_3$ ,  $\text{Cp}^*$ ). HRMS (ESI)  $m/z$  calculated for  $\text{C}_{23}\text{H}_{25}\text{ClIrN}_4$ : 585.1384 [M]<sup>+</sup>; found 585.1379. IR (KBr):  $\nu_{\text{max}}$  3059, 2969, 2920, 1614, 1497, 1482, 1383, 1091, 1029, 752, 697. Mp: decomposes before melting.

**Preparation of Rh-Complex 8.** To a solution of 28.9 mg (0.130 mmol, 1 equiv) of compound **3** in  $\text{CH}_2\text{Cl}_2$  (5 mL) were added 40 mg (0.065 mmol, 0.5 equiv) of  $[\text{RhCl}_2\text{Cp}^*]_2$  and 53.6 mg (0.156 mmol, 1.2 equiv) of  $\text{AgSbF}_6$ . After complete addition, the reaction was stirred under an argon atmosphere for 5 h. The solvent was decanted, and the resulting residue was washed with AcOEt ( $\times 3$ ) and vacuum-dried to yield the pure complex as an orange solid (87.6 mg, 92%).  $^1\text{H}$  NMR (400 MHz, acetonitrile- $d_3$ )  $\delta$  9.22 (s, 1H), 8.80 (dd,  $J = 5.5$ , 1.6 Hz, 1H), 8.38 (td,  $J = 8.0$ , 1.6 Hz, 1H), 8.05 (m, 3H), 7.83 (m, 1H), 7.58 (m, 3H), 1.79 (s, 15H).  $^{13}\text{C}$  NMR (101 MHz, acetonitrile- $d_3$ )  $\delta$  152.1 (C), 151.9 (CH), 146.4 (C), 144.0 (CH), 131.0 (CH), 130.3 (2CH), 128.9 (C), 128.0 (CH), 126.9 (2CH), 121.6 (CH), 115.1 (CH), 99.3 (SC, d,  $J_{\text{Rh,H}} = 8.6$  Hz,  $\text{Cp}^*$ ), 9.26 (5 $\text{CH}_3$ ,  $\text{Cp}^*$ ). HRMS (ESI)  $m/z$  calculated for  $\text{C}_{23}\text{H}_{25}\text{ClRhN}_4$ : 495.0817 [M]<sup>+</sup>; found 495.0811. IR (KBr):  $\nu_{\text{max}}$  3408, 1614, 1496, 1455, 1362, 1085, 895, 697, 660. Mp: decomposes before melting.

**Preparation of Complex 5.**  $[\text{IrCl}_2\text{Cp}^*]_2$  (19.3 mg, 0.024 mmol, 0.5 equiv) and  $\text{K}_2\text{CO}_3$  (13.4 mg, 0.097 mmol, 2.0 equiv) were added to a solution of complex **4** (30 mg, 0.048 mmol, 1.0 equiv) in 1,2-dichloroethane (9.0 mL), and the resulting mixture was refluxed under argon with good stirring for 18 h. After cooling, filtering through Celite, and removal of the solvent, the residue was purified by  $\text{SiO}_2$  column chromatography (3–5% MeOH in  $\text{CH}_2\text{Cl}_2$ ) to yield complex **5** as an orange solid (29.2 mg, 62%).  $^1\text{H}$  NMR (400 MHz,  $\text{CDCl}_3$ )  $\delta$  8.25 (dd,  $J = 7.2$ , 1.2 Hz, 1H), 8.08 (dd,  $J = 8.2$ , 1.4 Hz, 2H), 7.85 (dd,  $J = 5.6$ , 1.2 Hz, 1H), 7.42 (t,  $J = 7.7$  Hz, 2H), 7.30 (m,



1H), 6.98 (dd,  $J = 7.2, 5.6$  Hz, 1H), 1.79 (s, 15H), 1.59 (s, 15H).  $^{13}\text{C}$  NMR (101 MHz,  $\text{CDCl}_3$ )  $\delta$  159.3 (C), 155.5 (C), 147.8 (CH), 138.0 (C), 137.9 (CH), 135.4 (C), 134.2 (C), 128.2 (2CH), 127.8 (2CH), 127.3 (CH), 123.7 (CH), 90.0 (5C, Cp\*), 87.7 (5C, Cp\*), 9.38 (5CH<sub>3</sub>, Cp\*), 9.30 (5CH<sub>3</sub>, Cp\*). HRMS (ESI)  $m/z$  calcd for  $\text{C}_{33}\text{H}_{38}\text{ClIr}_2\text{N}_4$ : 911.2026 [M]<sup>+</sup>; found 911.2029. IR (KBr):  $\nu_{\text{max}}$  2914, 1502, 1447, 1381, 1203, 1075, 1033, 773, 700. Mp: decomposes before melting.

**Preparation of Complex 6.** To a solution of proligand **3** (14 mg, 0.063 mmol, 1.0 equiv) in MeCN (6.0 mL) were added  $[\text{IrCl}_2\text{Cp}^*]_2$  (50 mg, 0.063 mmol, 1.0 equiv) and NaOAc (10.3 mg, 0.126 mmol, 2.0 equiv). The resulting mixture was refluxed under argon with good stirring overnight. The residue was purified by  $\text{SiO}_2$  column chromatography (Hex:AcOEt, 2:8) to yield complex **6** as an orange solid (35 mg, 59%).  $^1\text{H}$  NMR (400 MHz,  $\text{CDCl}_3$ )  $\delta$  8.55 (d,  $J = 5.8$  Hz, 1H), 8.09 (d,  $J = 7.9$  Hz, 1H), 7.96 (tt,  $J = 8.4, 1.5$  Hz, 1H), 7.76 (m, 2H), 7.30 (t,  $J = 6.6$  Hz, 1H), 7.05 (t,  $J = 7.3$  Hz, 1H), 6.99 (t,  $J = 7.2$  Hz, 1H), 1.81 (s, 15H), 1.66 (s, 15H).  $^{13}\text{C}$  NMR (101 MHz,  $\text{CDCl}_3$ )  $\delta$  161.2 (C), 156.5 (C), 152.3 (C), 150.8 (CH), 140.5 (CH), 139.1 (C), 138.5 (C), 135.0 (CH), 127.8 (CH), 123.2 (CH), 122.1 (CH), 121.2 (CH), 112.8 (CH), 90.4 (5C, Cp\*), 88.7 (5C, Cp\*), 9.42 (5CH<sub>3</sub>, Cp\*), 9.32 (5CH<sub>3</sub>, Cp\*). HRMS (ESI)  $m/z$  calcd for  $\text{C}_{33}\text{H}_{38}\text{ClIr}_2\text{N}_4$ : 911.2026 [M]<sup>+</sup>; found 911.2044. IR (KBr):  $\nu_{\text{max}}$  2961, 2914, 2318, 1616, 1484, 1452, 1382, 1276, 771, 756. Mp: decomposes before melting.

**Preparation of Complex 9.**  $[\text{RhCl}_2\text{Cp}^*]_2$  (50 mg, 0.081 mmol, 1.0 equiv) and NaOAc (13.3 mg, 0.162 mmol, 2.0 equiv) were added to a solution of proligand **3** (18 mg, 0.081 mmol, 1.0 equiv) in MeCN (6.0 mL). The mixture was refluxed under argon for 6 h with good stirring. After cooling, filtering through Celite, and removal of the solvent, the residue was purified by  $\text{SiO}_2$  column chromatography (Hex:AcOEt, 2:8) to yield complex **9** as an orange solid (25.0 mg, 70%).  $^1\text{H}$  NMR (400 MHz,  $\text{CDCl}_3$ )  $\delta$  8.58 (d,  $J = 5.5$  Hz, 1H), 8.18 (d,  $J = 8.3$  Hz, 1H), 7.98 (m, 3H), 7.42 (t,  $J = 7.5$  Hz, 2H), 7.31 (m, 2H), 1.50 (s, 15H).  $^{13}\text{C}$  NMR (101 MHz,  $\text{CDCl}_3$ )  $\delta$  153.3 (C), 152.6 (C), 150.3 (CH), 140.6 (CH), 134.6 (2C), 128.5 (2CH), 128.4 (2CH), 127.4 (CH), 122.8 (CH), 113.0 (CH), 97.2 (5C, d,  $J_{\text{Rh,H}} = 6.8$  Hz, Cp\*), 9.45 (5CH<sub>3</sub>, Cp\*). HRMS (ESI)  $m/z$  calculated for  $\text{C}_{23}\text{H}_{24}\text{N}_4\text{Rh}$ : 459.1051 [M]<sup>+</sup>; found 459.1046. IR (KBr):  $\nu_{\text{max}}$  2963, 2915, 2220, 1613, 1486, 1468, 1228, 989, 774, 754. Mp: decomposes before melting.

**Preparation of Complex 10.**  $[\text{IrCl}_2\text{Cp}^*]_2$  (32.2 mg, 0.04 mmol, 0.5 equiv) and NaOAc (13.3 mg, 0.16 mmol, 2.0 equiv) were added to a solution of complex **9** (40.0 mg, 0.08 mmol, 1.0 equiv) in MeCN (6.0 mL). The resulting mixture was refluxed with good stirring under argon overnight. After cooling, filtration through Celite, and removal of the solvent, the residue was purified by  $\text{SiO}_2$  column chromatography (3–5% MeOH in  $\text{CH}_2\text{Cl}_2$ ) to yield complex **10** as an orange solid (30.0 mg, 43%).  $^1\text{H}$  NMR (400 MHz,  $\text{CDCl}_3$ )  $\delta$  8.60 (d,  $J = 4.8$  Hz, 1H), 8.07 (d,  $J = 8.2$  Hz, 1H), 7.99 (t,  $J = 8.4$ , 1H), 7.78 (t,  $J = 7.1$ , 2H), 7.36 (t,  $J = 7.2$  Hz, 1H), 7.07 (t,  $J = 7.4$ , 1H), 6.99 (t,  $J = 7.2$ , 1H), 1.80 (s, 15H), 1.61 (s, 15H).  $^{13}\text{C}$  NMR (100 MHz,  $\text{CDCl}_3$ )  $\delta$  162.5 (C), 156.6 (C), 152.0 (C), 151.6 (C), 150.7 (CH), 140.7 (CH), 138.6 (C), 135.2 (CH), 127.8 (CH), 123.1 (CH), 122.2 (CH), 121.4 (CH), 113.2 (CH), 97.7 (5C, d,  $J_{\text{Rh,H}} = 6.8$  Hz, Cp\*), 88.7 (5C, Cp\*), 9.65 (5CH<sub>3</sub>, Cp\*), 9.33 (5CH<sub>3</sub>, Cp\*). HRMS (ESI)  $m/z$  calcd for  $\text{C}_{33}\text{H}_{38}\text{ClIr}_2\text{N}_4$ : 821.1457 [M]<sup>+</sup>; found 821.1447. IR (KBr):  $\nu_{\text{max}}$  3436, 2914, 1613, 1481, 1381, 1271, 1020, 1002, 770, 734  $\text{cm}^{-1}$ . Mp: decomposes before melting.

**Crystallographic Data for Complexes 5, 6, and 9.** All data were collected at low temperature using oil-coated shock-cooled crystals at 110(2) K (**5**), 140(2) K (**6**), and 100(2) K (**9**) on a Bruker-AXS APEX II diffractometer with MoK $\alpha$  radiation ( $\lambda = 0.71073$  Å). The structures were solved by direct methods,<sup>22</sup> and all nonhydrogen atoms were refined anisotropically using the least-squares method on  $F^2$ .<sup>23</sup> The X-ray crystallographic data for **9**, **6**, and **5** have been deposited at the Cambridge Crystallographic Data Centre (CCDC) under deposition no. CCDC 2334796–2334798.

**5:**  $\text{C}_{33}\text{H}_{38}\text{Cl}_2\text{Ir}_2\text{N}_4$ ,  $M_r = 945.97$ , crystal size =  $0.30 \times 0.20 \times 0.20$  mm<sup>3</sup>, orthorhombic, space group  $Pbca$ ,  $a = 14.42(2)$  Å,  $b = 15.10(2)$

Å,  $c = 29.18(3)$  Å,  $V = 6354(11)$  Å<sup>3</sup>,  $Z = 8$ , 108,223 reflections collected, 9653 unique reflections ( $R_{\text{int}} = 0.0564$ ),  $R1 = 0.0478$ ,  $wR2 = 0.1009$  [ $I > 2\sigma(I)$ ],  $R1 = 0.0638$ ,  $wR2 = 0.1074$  (all data), residual electron density =  $4.243 \text{ e Å}^{-3}$ .

**6:**  $\text{C}_{35}\text{H}_{40}\text{Cl}_8\text{Ir}_2\text{N}_4$ ,  $M_r = 1184.71$ , crystal size =  $0.40 \times 0.10 \times 0.05$  mm<sup>3</sup>, monoclinic, space group  $P2_1/n$ ,  $a = 13.98(2)$  Å,  $b = 19.30(3)$  Å,  $c = 14.75(2)$  Å,  $\beta = 101.54(2)^\circ$ ,  $V = 3898(9)$  Å<sup>3</sup>,  $Z = 4$ , 53,647 reflections collected, 7707 unique reflections ( $R_{\text{int}} = 0.0633$ ),  $R1 = 0.0592$ ,  $wR2 = 0.1255$  [ $I > 2\sigma(I)$ ],  $R1 = 0.1050$ ,  $wR2 = 0.1537$  (all data), residual electron density =  $2.336 \text{ e Å}^{-3}$ .

**9:**  $\text{C}_{23}\text{H}_{24}\text{ClN}_4\text{Rh}$ ,  $M_r = 494.82$ , crystal size =  $0.30 \times 0.20 \times 0.05$  mm<sup>3</sup>, triclinic, space group  $P\bar{1}$ ,  $a = 8.761(1)$  Å,  $b = 14.373(1)$  Å,  $c = 17.402(1)$  Å,  $\alpha = 77.274(1)^\circ$ ,  $\beta = 81.430(2)^\circ$ ,  $\gamma = 82.967(2)^\circ$ ,  $V = 2104.4(1)$  Å<sup>3</sup>,  $Z = 4$ , 29,649 reflections collected, 8960 unique reflections ( $R_{\text{int}} = 0.0439$ ),  $R1 = 0.0484$ ,  $wR2 = 0.1391$  [ $I > 2\sigma(I)$ ],  $R1 = 0.0520$ ,  $wR2 = 0.1416$  (all data), residual electron density =  $1.416 \text{ e Å}^{-3}$ .

## ■ ASSOCIATED CONTENT

### Supporting Information

The Supporting Information is available free of charge at <https://pubs.acs.org/doi/10.1021/acs.organomet.4c00079>.

Copies of the  $^1\text{H}$  NMR,  $^{13}\text{C}$  NMR, and HRMS of the compounds prepared in this work (PDF)

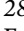
### Accession Codes

CCDC 2334796–2334798 contain the supplementary crystallographic data for this paper. These data can be obtained free of charge via [www.ccdc.cam.ac.uk/data\\_request/cif](http://www.ccdc.cam.ac.uk/data_request/cif), or by emailing [data\\_request@ccdc.cam.ac.uk](mailto:data_request@ccdc.cam.ac.uk), or by contacting The Cambridge Crystallographic Data Centre, 12 Union Road, Cambridge CB2 1EZ, UK; fax: +44 1223 336033.


## ■ AUTHOR INFORMATION

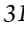
### Corresponding Authors

**María C. de la Torre** – Instituto de Química Orgánica General, Consejo Superior de Investigaciones Científicas (IQOG-CSIC), 28006 Madrid, Spain; Centro de Investigación en Química Avanzada (ORFEO–CINQA), Universidad Complutense, 28040 Madrid, Spain; Email: [mc.delatorre@csic.es](mailto:mc.delatorre@csic.es)

**Miguel A. Sierra** – Departamento de Química Orgánica I, Facultad de Química and Centro de Investigación en Química Avanzada (ORFEO–CINQA), Universidad Complutense, 28040 Madrid, Spain;  [orcid.org/0000-0002-3360-7795](https://orcid.org/0000-0002-3360-7795); Email: [sierraor@ucm.es](mailto:sierraor@ucm.es)

### Authors

**María Moreno-Latorre** – Instituto de Química Orgánica General, Consejo Superior de Investigaciones Científicas (IQOG-CSIC), 28006 Madrid, Spain; Centro de Investigación en Química Avanzada (ORFEO–CINQA), Universidad Complutense, 28040 Madrid, Spain;  [orcid.org/0000-0001-9033-7157](https://orcid.org/0000-0001-9033-7157)

**Heinz Gornitzka** – LCC–CNRS, Université de Toulouse, 31077 Toulouse Cedex 04, France;  [orcid.org/0000-0002-8838-5907](https://orcid.org/0000-0002-8838-5907)

**Catherine Hemmert** – LCC–CNRS, Université de Toulouse, 31077 Toulouse Cedex 04, France

Complete contact information is available at:

<https://pubs.acs.org/doi/10.1021/acs.organomet.4c00079>

### Author Contributions

M.A.S. and M.C.T. designed the work, M.A.S. and M.C.T. directed the research and interpreted the results, M.M.-L.



executed the experimental part and interpreted the experimental results, M.A.S. executed the DFT calculations, and H.G. and C.H. did the X-ray section of this paper. The manuscript was written through contributions of all authors.

## Notes

The authors declare no competing financial interest.

## ACKNOWLEDGMENTS

Support for this work under grants PID2022-139177OB-I00 (to MAS), PID2020-113662RB-I00 (to MCT), and RED2022-134287-T funded by MCIN/AEI/10.13039/501100011033 (Spain) is gratefully acknowledged. MMT thanks the MCIN for a predoctoral (FPI) grant.

## REFERENCES

- (1) Selected revisions: (a) Ryabov, A. D. Mechanisms of intramolecular activation of carbon-hydrogen bonds in transition-metal complexes. *Chem. Rev.* **1990**, *90*, 403–424. (b) Kakiuchi, F.; Murai, S. Activation of C–H Bonds: Catalytic Reactions. *Top. Organomet. Chem.* **1999**, *3*, 47–79. (c) Dyker, G. Transition Metal Catalyzed Coupling Reactions under C–H Activation. *Angew. Chem., Int. Ed.* **1999**, *38*, 1699–1712. (d) Colby, D. A.; Bergman, R. G.; Ellman, J. A. Rhodium-Catalyzed C–C Bond Formation via Heteroatom-Directed C–H Bond Activation. *Chem. Rev.* **2010**, *110*, 624–655. (e) Baudoin, O. Transition metal-catalyzed arylation of unactivated C(sp<sup>3</sup>)-H bonds. *Chem. Soc. Rev.* **2011**, *40*, 4902–4911.
- (2) (a) Scattergood, P. A.; Sinopoli, A.; Elliott, P. I. P. Photophysics and photochemistry of 1,2,3-triazole-based complexes. *Coord. Chem. Rev.* **2017**, *350*, 136–154. (b) Scattergood, P. A.; Elliott, P. I. P. An unexpected journey from highly tunable phosphorescence to novel photochemistry of 1,2,3-triazole-based complexes. *Dalton Trans.* **2017**, *46*, 16343–16356.
- (3) (a) Schulze, B.; Schubert, U. S. Beyond click chemistry-supramolecular interactions of 1,2,3-triazoles. *Chem. Soc. Rev.* **2014**, *43*, 2522–2571. (b) Jindabot, S.; Teerachanan, K.; Thongkam, K.; Kiattisevi, S.; Khamnaen, T.; Phiriyawirut, P.; Charoenchaidet, S.; Sooksimuang, T.; Kongsaree, P.; Sangtrirutnugul, P. Palladium(II) complexes featuring bidentate pyridine–triazole ligands: Synthesis, structures, and catalytic activities for Suzuki–Miyaura coupling reactions. *J. Organomet. Chem.* **2014**, *750*, 35–40. (c) Bertrand, H. C.; Clède, S.; Guillot, R.; Lambert, F.; Policar, C. Luminescence Modulations of Rhenium Tricarbonyl Complexes Induced by Structural Variations. *Inorg. Chem.* **2014**, *53*, 6204–6223. (d) Lo, W. K. C.; Huff, G. S.; Cubanski, J. R.; Kennedy, A. D. W.; McAdam, C. J.; McMorran, D. A.; Gordon, K. C.; Crowley, J. D. Comparison of Inverse and Regular 2-Pyridyl-1,2,3-triazole “Click” Complexes: Structures, Stability, Electrochemical, and Photophysical Properties. *Inorg. Chem.* **2015**, *54*, 1572–1587.
- (4) Selected examples: (a) Bertrand, H. C.; Clède, S.; Guillot, R.; Lambert, F.; Policar, C. Luminescence Modulations of Rhenium Tricarbonyl Complexes Induced by Structural Variations. *Inorg. Chem.* **2014**, *53*, 6204–6223. (b) Jindabot, S.; Teerachanan, K.; Thongkam, P.; Kiattisevi, S.; Khamnaen, T.; Phiriyawirut, P.; Charoenchaidet, S.; Sooksimuang, T.; Kongsaree, P.; Sangtrirutnugul, P. Palladium(II) complexes featuring bidentate pyridine–triazole ligands: Synthesis, structures, and catalytic activities for Suzuki–Miyaura coupling reactions. *J. Organomet. Chem.* **2014**, *750*, 35–40. (c) Guha, P. M.; Phan, H.; Kinyon, J. S.; Brotherton, W. S.; Sreenath, K.; Simmons, J. T.; Wang, Z.; Clark, R. J.; Dalal, N. S.; Shatruck, M.; Zhu, L. Structurally Diverse Copper(II) Complexes of Polyaza Ligands Containing 1,2,3-Triazoles: Site Selectivity and Magnetic Properties. *Inorg. Chem.* **2012**, *51*, 3465–3477. (d) Kuang, G.-C.; Michaels, H. A.; Simmons, J. T.; Clark, R. J.; Zhu, L. Chelation-Assisted, Copper(II)-Acetate-Accelerated Azide–Alkyne Cycloaddition. *J. Org. Chem.* **2010**, *75*, 6540–6548. (e) Urankar, D.; Pinter, B.; Pevec, A.; De Proft, F.; Turel, I.; Kosmrlj, J. Click-Triazole N2 Coordination to Transition-Metal Ions Is Assisted by a Pendant Pyridine Substituent. *Inorg. Chem.* **2010**, *49*, 4820–4829. (f) Kilpin, K. J.; Gavey, E. L.; McAdam, C. J.; Anderson, C. B.; Lind, S. J.; Keep, C. C.; Gordon, K. C.; Crowley, J. D. Gold(I) and Palladium(II) Complexes of 1,3,4-Trisubstituted 1,2,3-Triazol-5-ylidene “Click” Carbenes: Systematic Study of the Electronic and Steric Influence on Catalytic Activity. *Inorg. Chem.* **2011**, *50*, 6334–6346.
- (5) Valencia, M.; Müller-Bunz, H.; Gossage, R. A.; Albrecht, M. Enhanced product selectivity promoted by remote metal coordination in acceptor-free alcohol dehydrogenation catalysis. *Chem. Commun.* **2016**, *52*, 3344–3347.
- (6) (a) Frutos, M.; Avello, M. G.; Viso, A.; Fernández de la Pradilla, R.; de la Torre, M. C.; Sierra, M. A.; Gornitzka, H.; Hemmert, C. Gold Sulfinyl Mesoionic Carbenes: Synthesis, Structure, and Catalytic Activity. *Org. Lett.* **2016**, *18*, 3570–3573. (b) Frutos, M.; de la Torre, M. C.; Sierra, M. A. Steroid Derived Mesoionic Gold and Silver Mono- and Polymetallic Carbenes. *Inorg. Chem.* **2015**, *54*, 11174–11185.
- (7) Avello, M. G.; Frutos, M.; de la Torre, M. C.; Viso, A.; Velado, M.; Fernández de la Pradilla, R.; Sierra, M. A.; Gornitzka, H.; Hemmert, C. Chiral Sulfur Functional Groups as Definers of the Chirality at the Metal in Ir and Rh Half-Sandwich Complexes: A Combined CD/X-ray Study. *Chem. – Eur. J.* **2017**, *23*, 14523–14531.
- (8) Avello, M. G.; de la Torre, M. C.; Sierra, M. A.; Gornitzka, H.; Hemmert, C. Central (S) to Central (M = Ir, Rh) to Planar (Metallocene, M = Fe, Ru) Chirality Transfer Using Sulfoxide-Substituted Mesoionic Carbene Ligands: Synthesis of Bimetallic Planar Chiral Metallocenes. *Chem. – Eur. J.* **2019**, *25*, 13344–13353.
- (9) (a) Bolje, A.; Urankar, D.; Kosmrlj, J. Synthesis and NMR Analysis of 1,4-Disubstituted 1,2,3-Triazoles Tethered to Pyridine, Pyrimidine, and Pyrazine Rings. *Eur. J. Org. Chem.* **2014**, *2014*, 8167–8181. (b) Chattopadhyay, B.; Rivera Vera, C. I.; Chuprakov, S.; Gevorgyan, V. Fused Tetrazoles as Azide Surrogates in Click Reaction: Efficient Synthesis of N-Heterocycle-Substituted 1,2,3-Triazoles. *Org. Lett.* **2010**, *12*, 2166–2169.
- (10) DFT calculations at b3lyp-lanl2dz gd3 level in vacuo (see the experimental section for computational details).
- (11) The relationship between the values of d and the acidity has been established following several approaches, mostly based on free-energy relationships and computational methods. We have chosen the approach reported by Penhoat in a) Penhoat, M. Scope and Limitations of a <sup>1</sup>H NMR Method for the Prediction of Substituted Phenols pK<sub>a</sub> Values in water, CH<sub>3</sub>CN, DMF, DMSO and i-PrOH. *Tetrahedron Lett.* **2013**, *54*, 2571–2574. We used the equation pK<sub>a</sub>(CH<sub>3</sub>CN) = −3.149 × dOH + 55.91 due to its excellent correlation factor.
- (12) Reaction conditions analogous to the used with [IrCp\*Cl<sub>2</sub>]<sub>2</sub> to prepare complex **4** resulted in the recovery of unreacted starting materials. The reaction in boiling DCM also resulted in the recovery of the unaltered starting materials. These differences in reactivity between [RhCp\*Cl<sub>2</sub>]<sub>2</sub> and [IrCp\*Cl<sub>2</sub>]<sub>2</sub> have been repeatedly observed. The lower reactivity of [RhCp\*Cl<sub>2</sub>]<sub>2</sub> compared to [IrCp\*Cl<sub>2</sub>]<sub>2</sub> has been attributed to the lower electrophilicity of the Rh complex. Examples: (a) Li, L.; Brennessel, W. W.; Jones, W. D. C–H Activation of phenyl imines and 2-phenylpyridines with [Cp\*MCl<sub>2</sub>]<sub>2</sub> (M = Ir, Rh): regioselectivity, kinetics, and mechanism. *Organometallics* **2009**, *28*, 3492–3500. (b) Zhang, S.; Chu, X.; Li, T.; Wang, Z.; Zhu, B. Synthesis, structures, and reactivity of single and double cyclometalated complexes formed by reactions of [Cp\*MCl<sub>2</sub>]<sub>2</sub> (M = Ir and Rh) with dinaphthyl phosphines. *ACS Omega* **2018**, *3*, 4522–4533. (c) Zhao, C.; Ge, Q.; Wang, B.; Xu, V. Comparative investigation of the reactivities between catalysts [Cp\*RhCl<sub>2</sub>]<sub>2</sub> and [Cp\*IrCl<sub>2</sub>]<sub>2</sub> in the oxidative annulation of isoquinolones with alkynes: a combined experimental and computational study. *Org. Chem. Front.* **2017**, *4*, 2327–2335.
- (13) (a) Lionetti, D.; Day, V. W.; Blakemore, J. D. Synthesis and Electrochemical Properties of Half-Sandwich Rhodium and Iridium Methyl Complexes. *Organometallics* **2017**, *36*, 1897–190. (b) Valencia, M.; Martín-Ortiz, M.; Gómez-Gallego, M.; Ramírez de Arellano, C.; Sierra, M. A. On the Use of Metal Purine Derivatives (M = Ir, Rh)

for the Selective Labeling of Nucleosides and Nucleotides. *Chem. – Eur. J.* **2014**, *20*, 3831–3838. (c) Blakemore, J. D.; Schley, N. D.; Balcells, D.; Hull, J. F.; Olack, G. W.; Incarvito, C. D.; Eisenstein, O.; Brudvig, G. W.; Crabtree, R. H. Half-Sandwich Iridium Complexes for Homogeneous Water-Oxidation Catalysis. *J. Am. Chem. Soc.* **2010**, *132*, 16017–16029. (d) Tamayo, A. B.; Alleyne, B. D.; Djurovich, P. I.; Lamansky, S.; Tsyba, I.; Ho, N.; Bau, R.; Thompson, M. E. Synthesis and Characterization of Facial and Meridional Tris-cyclometalated Iridium(III) Complexes. *J. Am. Chem. Soc.* **2003**, *125*, 7377–7387.

(14) (a) Fan, S.; Zong, X.; Shaw, P. E.; Wang, X.; Geng, Y.; Smith, A. R. G.; Burn, P. L.; Wang, L.; Lo, S.-C. Energetic requirements of iridium(III) complex based photosensitisers in photocatalytic hydrogen generation. *Phys. Chem. Chem. Phys.* **2014**, *16*, 21577–21585. (b) DiLuzio, S.; Connell, T. U.; Mdluli, V.; Kowalewski, J. F.; Bernhard, S. Understanding Ir(III) Photocatalyst Structure–Activity Relationships: A Highly Parallelized Study of Light-Driven Metal Reduction Processes. *J. Am. Chem. Soc.* **2022**, *144*, 1431–1444.

(15) Si-Hai Wu, S.-H.; Shen, J. J.; Yao, J.; Zhong, Y. W. Asymmetric Mixed-Valence Complexes that Consist of Cyclometalated Ruthenium and Ferrocene: Synthesis, Characterization, and Electronic-Coupling Studies. *Chem. – Asian J.* **2013**, *8*, 138–147. and the pertinent references therein

(16) Stengel, I.; Mishra, A.; Pootrakulchote, N.; Moon, S.-J.; Zakeeruddin, S. M.; Grätzel, M.; Bäuerle, P. Click-chemistry” approach in the design of 1,2,3-triazolyl-pyridineligands and their Ru(II)-complexes for dye-sensitized solar cells. *J. Mater. Chem.* **2011**, *21*, 3726–3734.

(17) (a) Lee, C.; Yang, W.; Parr, R. G. Development of the Colle-Salvetti correlation-energy formula into a functional of the electron density. *Phys. Rev. B* **1988**, *37*, 785–789. (b) Becke, A. D. Density-functional thermochemistry. III. The role of exact exchange. *J. Chem. Phys.* **1993**, *98*, 5648–5652. (c) Stephens, P. J.; Devlin, F. J.; Chabalowski, C. F.; Frisch, M. J. Ab Initio Calculation of Vibrational Absorption and Circular Dichroism Spectra Using Density Functional Force Fields. *J. Phys. Chem.* **1994**, *98*, 11623–11627.

(18) Frisch, M. J.; Trucks, G. W.; Schlegel, H. B.; Scuseria, G. E.; Robb, M. A.; Cheeseman, J. R.; Scalmani, G.; Barone, V.; Petersson, G. A.; Nakatsuji, H. et al. *Gaussian 16, Revision C.01*; Gaussian, Inc.: Wallingford CT, 2016.

(19) Grimme, S.; Antony, J.; Ehrlich, S.; Krieg, H. A consistent and accurate ab initio parametrization of density functional dispersion correction (DFT-D) for the 94 elements H–Pu. *J. Chem. Phys.* **2010**, *132*, 154104.

(20) Hay, P. J.; Wadt, W. R. Ab initio effective core potentials for molecular calculations – potentials for K to Au including the outermost core orbitals. *J. Chem. Phys.* **1985**, *82*, 299–310.

(21) (a) Bolje, A.; Urankar, D.; Kosmrlj, J. Synthesis and NMR Analysis of 1,4-Disubstituted 1,2,3-Triazoles Tethered to Pyridine, Pyrimidine, and Pyrazine Rings. *Eur. J. Org. Chem.* **2014**, *2014*, 8167–8181. (b) Chattopadhyay, B.; Rivera Vera, C. I.; Chuprakov, S.; Gevorgyan, V. Fused Tetrazoles as Azide Surrogates in Click Reaction: Efficient Synthesis of N-Heterocycle-Substituted 1,2,3-Triazoles. *Org. Lett.* **2010**, *12*, 2166–2169.

(22) Sheldrick, G. M. A short history of SHELX. *Acta Crystallogr.* **2008**, *A64*, 112–122.

(23) Sheldrick, G. M. Crystal structure refinement with SHELXL. *Acta Crystallogr.* **2015**, *C71* (1), 3–8.